




Article

Graphene–Silver Hybrid Nanoparticle based Organic Phase Change Materials for Enhanced Thermal Energy Storage

B. Kalidasan ¹, A. K. Pandey ^{1,2,*}, Saidur Rahman ^{1,2}, Aman Yadav ³, M. Samykano ³ and V. V. Tyagi ⁴

¹ Research Centre for Nano-Materials and Energy Technology (RCNMET), School of Engineering and Technology, Sunway University, No. 5, Jalan Universiti, Bandar Sunway, Petaling Jaya 47500, Selangor Darul Ehsan, Malaysia

² Sunway Materials Smart Science and Engineering (SMS2E) Research Cluster, Sunway University, No. 5, Jalan Universiti, Bandar Sunway, Petaling Jaya 47500, Selangor, Malaysia

³ College of Engineering, University Malaysia Pahang, Lebuhraya Tun Razak, Gambang, Kuantan 26300, Pahang, Malaysia

⁴ School of Energy Management, Shri Mata Vaishno Devi University, Katra 182320, Jammu & Kashmir, India

* Correspondence: adarshp@sunway.edu.my

Abstract: Due to the intermittent nature of solar energy, researchers and scientists are working to develop thermal energy storage (TES) systems for effective utilization of solar energy. Phase change materials (PCMs) are considered to be promising materials for TES. In this study, organic paraffin RT50 and graphene silver (Gr:Ag) nanopowder are adopted as TES material and thermal property enhancers. Microstructure and morphological behavior as well as chemical, optical, and thermal stability of the prepared composite PCM are visually investigated using scanning electron microscope (SEM), energy dispersive X-ray spectroscopy (EDX), Fourier transform infrared spectroscopy (FT-IR), UV-Vis spectroscopy, thermal conductivity analyzer, differential scanning calorimeter (DSC) and thermogravimetric analyzer (TGA). Furthermore, based on the outstanding thermal performance of the composite, an extended investigation on the thermal and chemical properties are evaluated for 500 thermal cycles to ensure their reliability. Results show the thermal conductivity of RT50 improved by 53.85% when Gr:Ag nanopowder is dispersed at a weight percent of 0.8 (RT50-0.8Gr:Ag). The change in latent heat value of the composite sample is less than 3%, which is significant for effective thermal energy storage. The thermal decomposition of RT50 is slightly improved from 300 °C to 330 °C. To ensure a reliable and passive technique for thermal energy storage within solar thermal application devices, such as solar air heaters and solar photovoltaic thermal systems, using nanoparticle enhanced PCMs at the range of a 50 °C melting point are a current research hotspot.

Keywords: organic PCMs; hybrid nanoparticle; graphene:silver; thermal energy storage; solar energy; thermal stability



check for updates

Citation: Kalidasan, B.; Pandey, A.K.; Rahman, S.; Yadav, A.; Samykano, M.; Tyagi, V.V. Graphene–Silver Hybrid Nanoparticle based Organic Phase Change Materials for Enhanced Thermal Energy Storage. *Sustainability* **2022**, *14*, 13240. <https://doi.org/10.3390/su142013240>

Academic Editor: Mariateresa Lettieri

Received: 25 August 2022

Accepted: 10 October 2022

Published: 14 October 2022

Publisher's Note: MDPI stays neutral with regard to jurisdictional claims in published maps and institutional affiliations.



Copyright: © 2022 by the authors. Licensee MDPI, Basel, Switzerland. This article is an open access article distributed under the terms and conditions of the Creative Commons Attribution (CC BY) license (<https://creativecommons.org/licenses/by/4.0/>).

1. Introduction

The global energy system predominantly demands conventional fossil fuels due to the rapid advancement in human society. Security of energy and climate change are major critical problems worldwide as conventional fossil fuels are non-renewable and are on the verge of extinction. With high fossil fuels consumption, the environment becomes more polluted causing a rise in atmospheric temperature [1]. To reduce consumption of traditional fossil fuels, adequate thermal energy storage (TES) systems are currently required to store heat from solar energy sources, as solar power is intermittent in nature. Hence, we must find a suitable energy storage system to store thermal energy for use during late sunshine hours. TES is an ecologically sustainable energy storage [2] technique, which protects the environment and reduces dependency on fossil fuels. Phase change materials (PCMs) are the best suited materials based on ideal properties to store solar thermal energy during the phase change process. PCMs are classified into three categories: (a) organic

PCMs, (b) in-organic PCMs, and (c) eutectic PCMs. Organic PCMs have outstanding properties for storing thermal energy with a wide melting range without any supercooling issue [3]. In contrast, they face certain disadvantages, such as low thermal conductivity, being flammable, and poor light absorption properties. These disadvantages are barriers to the practical application of PCMs in solar–thermal application systems [4,5]. Nanoparticles such as graphite foam [6], graphene aerogels [7], carbon nanotube sponge [8], biomass carbon, and organic dyes [9,10] are introduced as a supporting matrix for fabricating composite PCMs to increase the thermal stability [11,12], light-absorbing capabilities [13], mechanical properties [14], preventing leakage problems, and a high specific surface area [13]. Moreover, nanoparticles can enhance the surface area to volume ratio and reduce the phase change rate. Dispersing high-thermal-conductive nanoparticles into a PCM offers an optimistic solution for enhancing a solution's thermal conductivity and thermal efficiency [15]. Thus, nano-enhanced organic PCMs are considered the most capable materials for storing energy, which is superior when compared to the limitations of PCMs [16]. Thermal conductivity of nano-enhanced organic PCMs is controlled by the nanoparticles and their interactional compatibility [17].

Numerous research investigations have been carried out to enhance the thermal property of different PCMs using graphene as a nanoparticle. Outstanding research works in regard to graphene nanoparticles and organic PCMs are discussed below to identify the research gap. Abdelrazik et al. [18] experimentally examined the thermal performance of paraffin wax with graphene nanoplatelets (GnP) at 0.1%, 0.5%, 1%, and 5% of mass fraction. The focus of the study was to enhance thermal conductivity of paraffin wax (PW) using GnP nanoparticles. Thermal conductivity of the PW/GnP composite was enhanced by 3.8% at 25 °C as the GnP nanoparticle with higher thermal property develops well-established thermal pathways. Li et al. [19] investigated using polyethylene glycol (PEG) as the PCM material and dispersion graphene oxide (GO) as the nanoparticle for superior solar thermal energy conversion. Latent heat of PEG/GO-PAM composite is 162.8 J/g after 1000 thermal cycles and their solar–thermal efficiency is 93.7%. Laghari et al. [2] characterized the thermal properties of PW/TiO₂-Gr composites with 0.1%, 0.5%, 1%, and 2% mass fraction of TiO₂-Gr as the nanoparticle. Latent heat of PW/TiO₂-Gr composite was increased by 10.02% at 1:1 of a TiO₂-Gr compared with the base PCM (RT-47). Thermal conductivity of PW/TiO₂-Gr composite increased by 179% at 1:1 of a TiO₂: Gr compared with base PCM. Vivekananthan [20] investigated the thermophysical characteristics of erythritol PCM with 0.1%, 0.5%, and 1.0% mass fraction of graphene nanoparticles. Results depicted increase in thermal conductivity (1.074 W/mK, 1.095 W/mK, and 1.122 W/mK) of the composites with increasing in concentration (0.1%, 0.5%, and 1%) of nanoparticles as compared with pure PCM due to uniform dispersion and active formation of thermal networks. Liu et al. [21] conducted research investigation to characterize the thermal properties of RT-70 with GnP nanoparticles. GnP dispersion nanocomposites with 0.2% and 2 wt% were prepared in their investigation. Their results showed an increase in thermal conductivity of base PCM from 0.268 W/mK to 0.326 W/mK at 0.2% of GnP, whereas with 2% of GnP the nanoparticles tend to agglomerate and resulted in settling without proper thermal networks. Tariq et al. [22] investigated the effect of graphene nanoparticles with two different commercial PCMs, RT-44 and RT-64. Graphene nanoparticles were included at 0.002, 0.005, and 0.008 wt%. In this study the authors explored the charging and discharging rate of the composite PCM with different heat input power supply of 0.86 KW/m², 1.44 KW/m², and 2.40 KW/m². It was noted that after 90 min of charging of the composite samples with 0.008 wt% nanoparticle concentration and 0.86 KW/m², the base temperature of 44 HC/GNPs reduced by 23%, whereas the 64 HC/GNPs composite base temperature was reduced by 7.2%. Pasupathi et al. [23] analyzed the variation of thermophysical properties of paraffin wax under the influence of hybrid nanoparticles containing an equal mass of SiO₂ and CeO₂ nanoparticles. Results ensured increase in thermal stability of the composite PCM, without much drop in latent heat value.

Pradeep et al. [24] experimentally investigated the performance of PW with silver nanoparticles at 0.05% and 0.1% concentrations. In their work, an effort was made to investigate the change in melting and solidification temperature of the base PCM with silver nanoparticle. Results showed the variation in the average temperature between rise and fall are within the limit of 11% and 29.5% for 0.05% and 0.1% concentrations, respectively. Prabhu and Valanarasu [25] analyzed the thermal stability and performance of paraffin using TiO₂-Ag nanoparticles synthesized using a ball milling process. Results show that the thermal conductivity of TiO₂-Ag/paraffin composite with a surfactant is improved and the latent heat capacity is also improved. Out of all the surfactant SDS, a surfactant is most suitable for latent heat capacity and thermal ability as it increases the particle-to-particle interactions with inclusion of a nanoparticle. Zhan et al. [26] experimentally investigated two-dimensional montmorillonite (2D-Mt) nanosheets as they could be exfoliated to sheet for proper dispersion of nanoparticles, phase stability, and enhanced thermal performance. The PCM used for the investigation was stearic acid and the nanoparticle was silver. Ag nanoparticle included in the core was stearic acid and in the shell was 2D-Mt, which were vital in enhancing the thermal conductivity of the composite sample. Results showed the latent heat of a 2D-Mt/SA/Ag to be 187 J/g at a 90% weight fraction of SA and the thermal conductivity of a 2D-Mt/SA/Ag increased by 229.3% during Ag nanoparticle dispersion into PCM core. Additionally, the 2D-Mt/SA/AgN composite exhibited an excellent photothermal conversion efficiency and enhanced thermal stability. Wen et al. [27] investigated the thermal properties of lauric acid PCM by dispersing hybrid silver-expanded graphite (Ag-EG) nanoparticles. Ag-EG/LA was prepared using vacuum impregnation. The results showed thermal conductivity and latent heat of the Ag-EG/LA composite to be 129.5 J/g and 2.85 W/mK at 47.2 °C. Thermal characteristic investigation of a composite shape stabilized PCM prepared using PEG and silver nanoparticle was carried out by Qian et al. [28]. To enhance the pore size and to improve the surface area, the PEG PCM was diatomite made using alkali leaching, followed by dispersion of silver nanoparticles. Results showed that the thermal conductivity of PEG/diatomite/Ag composite (0.82 W/mK) to increase by 127% at 7.5% concentration of Ag and the enthalpy of PEG/diatomite/Ag composite to reach 111.3 J/g. The prepared composite PCM is ensured to be thermally stable after 200 thermal cycles of charging and discharging thermal energy. Luo et al. [29] melted and blended polyethylene glycol (PEG) and epoxy resin (EP) to prepare a form-stable PCM. EF-Ag nanoparticles were dispersed with the prepared form stable PCM to enhance their thermophysical properties. Results showed that the thermal conductivity of the composite PCM increased by 121% and the photothermic efficiency increased by 90.7% with a 4% mass fraction of EG-Ag nanoparticle, in comparison to the pure PEG-EP PCM. Li et al. [30] investigated the thermal conductivity and the energy storage density of the rGO-Co/PEG composite. In this experiment, rGO-Co/PEG composites were prepared with the help of the physical mixing and melt impregnation method using PEG2000. It was noted that the thermal conductivity of rGO-Co/PEG composites increased by 51.79~152.46% compared with pure PEG. Additionally, the storage density is 131.94 J/g, which provides good stability and increases the heat storage rate.

Though numerous research works have been carried out with a focus on enhancing the thermophysical properties of organic and inorganic PCMs with metal and carbon nanoparticles individually, there is a research gap on the influence of hybrid nanoparticles with medium temperature PCMs. Metal additives are much denser and cause settling of nanoparticles; in contrast, a few carbon-based nanoparticles exhibit lower density and tends to float. Nevertheless, to take advantage of the high thermal conductivity of carbon nanoparticles and the higher density of metal nanoparticles, we have worked to explore the nature of hybridized carbon metal nanoparticles for thermal energy storage of PCMs.

Preferably PCMs are used for thermal energy storage, based on the temperature range of heat generation units. For example, for buildings, a cooling PCM with a melting point of 25–28 °C is selected; for a solar cooker, a PCM with melting point of 80–130 °C is selected. In this regard, as the current investigation is related to heat extraction from solar thermal

system generating heat at the temperature range of 45–60 °C, we have opted for a PCM with a melting temperature of 50 °C. Organic PCMs are superior to inorganic PCMs in terms of degree of supercooling; therefore, in this study we have opted for a commercial organic PCM, RT50, with a melting point of 50 °C. Favorable properties of silver nanoparticles and graphene nanoparticles have attracted many researchers to conduct numerous thermal studies. Here, a hybrid combination of Gr:Ag is used to enhance the energy storage characteristics of organic PCM for encouraging the research studies. In this study considering the promising nature of a Gr and Ag nanoparticle, a hybrid of both in a 1:1 ratio is used to enhance the thermal property of the commercial organic PCM RT50. To uniformly disperse Gr:Ag nanoparticles with RT50 PCM and to maintain the layered structure of Gr nanoparticles and spherical shape of Ag nanoparticle, the water bath sonication technique was adopted. We have characterized Gr:Ag nanoparticle dispersed sample at concentrations of 0.2%, 0.4%, 0.6%, 0.8%, and 1.0% using SEM, EDS, FTIR, UV-Vis, Tempos, DSC, and TGA to understand the chemical and thermal nature. Microstructure, morphological behavior, and compatibility of the composite samples were initially investigated using SEM and FTIR instruments. In addition, the thermal characteristics such as thermal conductivity, latent heat of melting, and decomposition temperature were analyzed using TEMPOS, DSC, and TGA instruments. The thermal cycling nature of the sample was also studied for up to 500 cycles and the chemical and thermal reliability of the samples were analyzed to ensure their reliability.

2. Materials and Methodology

2.1. Material Specifications

To assist the thermal management of batteries, commercial PCM RT50 belonging to the paraffin group with a phase transition temperature of 50 °C were acquired from RUBITHERM, Germany, for the experiments. PCM RT50 selected replicates excellent heat storage enthalpy of 160 J/g, without any effect of supercooling. Graphene silver nanopowder (Gr:Ag, 1:1) was procured from US Research Nanomaterials, Inc. to further enhance the thermal conductivity of the PCM RT50. The silver nanopowder in the above hybrid nanoparticle prevents the reagglomerating of the dispersed graphene nanoparticle and shows synergistic effect with Gr. The thermophysical properties of RT50 and Gr:Ag (1:1) nanopowder used in the research are represented in Table 1.

Table 1. Thermophysical characteristics of materials used in this study.

Properties	PCM	Nano Powder	
	RT 50	Graphene (Gr)	Silver (Ag)
Phase Transition Temperature	50 °C	3550 °C	961.8 °C
Thermal Conductivity	0.2 W/mK	4000 W/mK	429 W/mK
Heating Enthalpy	160 kJ/kg	-	-
Density	880 kg/m ³	130 kg/m ³	10,500 kg/m ³
Particle Size	-	1– μ m	20 nm
Color	White	Black	Black
Purity	-	>99 wt%	99.99%
Surface Area	-	500–1200 m ² /g	18–22 m ² /g

2.2. Preparation of Nanocomposite PCM

An organic solid PCM RT50 of 25 gm was weighed using analytical microbalance (EX224, OHAUS) and taken in a sample bottle. The PCM sample was then heated to 70 °C using a hot plate (RCT, BASIC IKA) to transform the solid PCM into liquid PCM, for uniform dispersion of nanoparticles. Graphene silver nanopowder was dispersed to the organic PCM RT50 at weight concentrations of 0.2 wt%, 0.4 wt%, 0.6 wt%, 0.8 wt%, and 1.0 wt%. A nanoparticle of 0.05 gm was added to 24.95 gm of RT50 PCM to prepare the RT50-0.2Gr:Ag composite sample. The samples were sonicated using ultrasonic bath (EASY 60H, ELMASONIC) for 60 min for uniform dispersion. Likewise the RT50-0.4Gr:Ag,

RT50-0.6Gr:Ag, RT50-0.8Gr:Ag, and RT50-1.0Gr:Ag composite PCMs were prepared for further experimental characterization. Figure 1 shows the step-by-step procedure followed for preparing the nanocomposite samples with different weight concentrations of graphene silver nanopowder.



Figure 1. Preparation of RT50-Gr:Ag composite PCM using bath ultrasonicator.

2.3. Instruments and Characterizations

Morphology of the nanoparticle dispersed composite organic PCM was visually investigated using a scanning electron microscope (SEM) TESCAN VEGA 3 (NOVATI SCIENTIFIC, Selangor, Malaysia) equipped with the VEGAS software. The SEM instrument is also attached to an energy dispersive X-ray spectroscopy (EDX) (Oxford Instruments, UK). Chemical characteristics of the developed nanocomposite PCM were characterized by FTIR (PERKIN ELMER, Los Angeles, California, USA), and a wavenumber range of $400\text{--}4000\text{ cm}^{-1}$ was used to determine the functional groups and chemical composition. An optical absorbance and transmittance were examined by using UV-Vis spectroscopy (PERKIN ELMER, Los Angeles, California, USA). The readings were taken at wavelength $280\text{--}1400\text{ nm}$ at room temperature. The thermal properties, such as thermal conductivity, were analyzed using thermal property analyzer (TEMPOS) dual needle SH-3 at normal room temperature. A thermogravimetric analyzer (TGA) (Perkin Elmer TGA 4000) was used to conduct a thermal deterioration analysis on pure PCM and the composite PCM with Gr:Ag nanoparticle. The temperature for TGA was ramped up to $350\text{ }^{\circ}\text{C}$ at a rate of $10\text{ }^{\circ}\text{C}/\text{min}$ in a N_2 environment. Differential scanning calorimetry (DSC) (DSC 3500 Sirius, NETZSCH, Selangor, Malaysia) was used to analyze the melting temperature and latent heat properties of composite PCM. DSC melting curves were inspected between $20\text{ }^{\circ}\text{C}$ and $80\text{ }^{\circ}\text{C}$ under the N_2 atmosphere with a heating rate of $5\text{ }^{\circ}\text{C}/\text{min}$. Thermal cycle tester instrument is used to ensure the thermal stability of the prepared samples. The samples were tested for heating and cooling between the temperatures of $30\text{ }^{\circ}\text{C}$ to $70\text{ }^{\circ}\text{C}$ at $15\text{ }^{\circ}\text{C}/\text{min}$ under static environmental conditions.

3. Results and Discussion

3.1. Microstructure and Composition Analysis Using SEM and EDX

The SEM image in Figure 2 represents the morphology, microstructure of PCM (RT50), nanoparticle (Gr:Ag), and the composite PCM (RT50-0.8GrAg). The commercial organic PCM RT50 used for the current study is visualized using SEM, as shown in Figure 2a, to ensure their morphology characteristics. RT50 PCM replicates a similar morphological image to that of paraffin. In Figure 2b, layered graphene particles of $1\text{--}2\text{ }\mu\text{m}$ are clearly compared with the nanosized silver nanoparticles. A hybrid mixture of Gr:Ag is of equal proportion with special silver nanoparticles filling the voids and pores of graphene ensuring a uniform blend. Figure 2c shows the morphological image of composite PCM with 0.8% mass fraction of Gr:Ag nanoparticle. A well-dispersed mixture of Gr:Ag is

observed with RT50 organic PCM. For better understanding, the digital images of RT50 and RT50-0.8GrAg, in the form of solid pellets, are depicted in Figure 2d. Additionally, to ensure the chemical composition of the PCMs, nanoparticle, and composite PCMs, they are visualized under EDX spectroscopy and the spectrums are indicated in Figure 3. As graphene is a compound of carbon, the spectrum of Gr:Ag indicates the presence of C and Ag elements in Figure 3a. Organic PCM RT50 is a compound of carbon, and in Figure 3b the C elements are replicated when visualized using EDX spectroscopy. The composite PCM in Figure 3c indicates the dispersion of Gr:Ag nanoparticles in a uniform fashion and confirms its presence in the prepared composite sample.

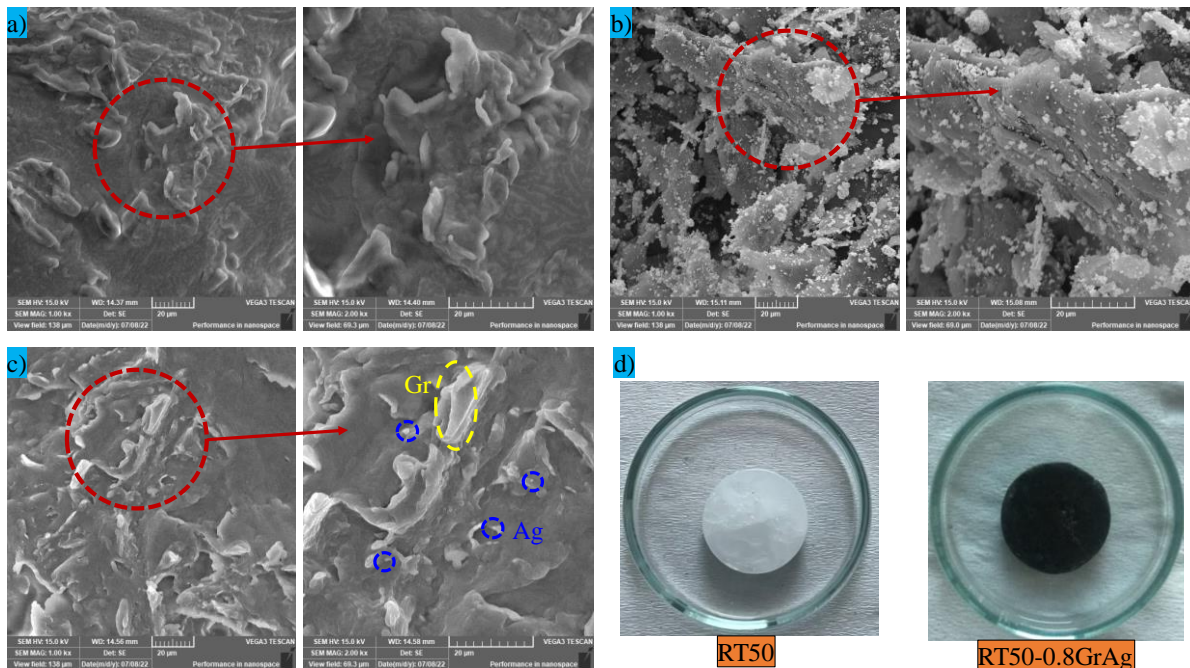


Figure 2. Morphological SEM image of (a) RT50, (b) graphene silver nanoparticle, (c) RT50 with 0.8% mass fraction of Gr:Ag nanoparticle, and (d) digital image of pure and composite PCMs.

3.2. Chemical Stability Investigation Using FTIR

Prepared composite PCMs are evaluated using FTIR spectrometry to analyze the chemical stability by identification of functional groups. Figure 4 shows the FTIR spectral curve of a graphene silver nanopowder dispersed organic PCM. When IR rays occur, the paraffin molecule exhibits four IR active vibrations modes at wavenumber 721 cm^{-1} , 1465 cm^{-1} , 2850 cm^{-1} , and at 2916 cm^{-1} , as shown in Figure 4. Peak 721 cm^{-1} represents the rocking mode vibration of $-\text{CH}_2$ groups, where an angular bending of bonds occurs. Peak 1465 cm^{-1} indicates the deformation of $-\text{CH}_2$ and $-\text{CH}_3$. Peak 2850 cm^{-1} and 2916 cm^{-1} indicate the symmetrical stretching vibration of $-\text{CH}_2$ and $-\text{CH}_3$ [31]. As the nanopowder Gr:Ag does not have a carboxyl group attached, they are not IR active and do not generate any peak on occurrence of IR rays. All the organic PCM composites with different weight concentration of Gr:Ag show similar spectral curves to that of pure RT50 (paraffin), which indicates that the nanopowder and the PCM are mixed physically, and no other chemical reactions take place and also ensure good compatibility of the prepared organic composite PCM.

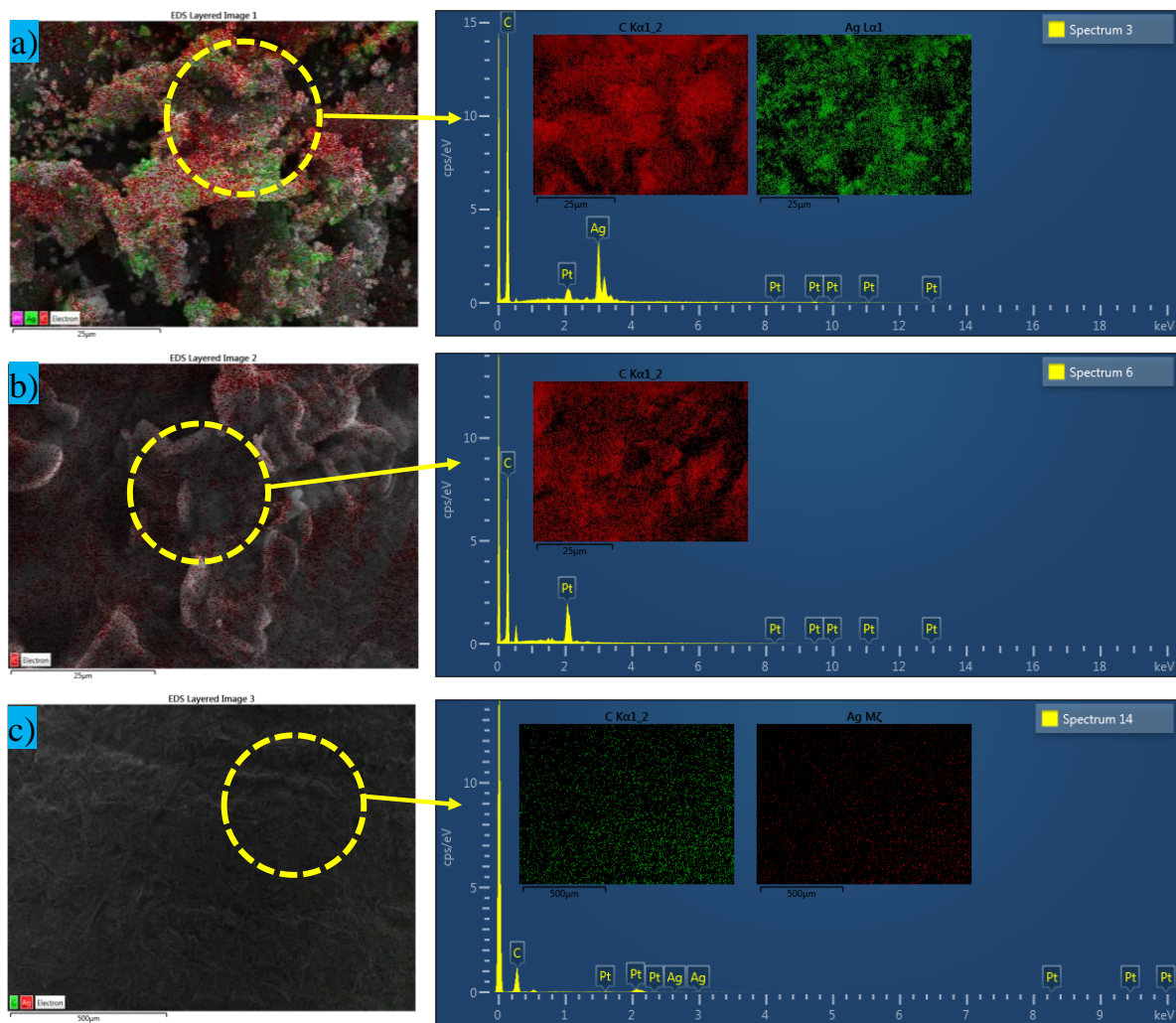


Figure 3. EDX spectrum composition of (a) graphene silver nanoparticle, (b) RT50 PCM, and (c) RT50 with 0.8% mass fraction Gr:Ag nanoparticle.

3.3. UV-Vis Analysis

Phase change materials are widely preferable for storing thermal energy. Solar power is the major source of thermal energy in the form of electromagnetic waves. The PCM used for energy storage are important to replicate high solar radiations absorption potential. In general, all organic materials are transparent in nature with high transmissibility. The nanoparticles dispersed with the PCM are expected to enhance the absorptivity of an organic PCM; therefore, enhancing the optical property of the PCM to absorb solar energy readily. Using UV-VIS spectrum analysis, a monochromatic beam of light rays is passed through the organic solid PCM specimen in order to assess the absorbance and transmissibility. Figures 5 and 6 indicate the absorbance and transmissibility of the base RT50 PCM sample and the Gr:Ag nanopowder dispersed composite PCM sample with the wavelength range of 280–1400 nm, as major solar radiation are under the UV region (280–380 nm), visible region (380–740 nm), and near-IR region (740–1400 nm). From Figure 5 it is clearly evident that the absorbance of base RT50 PCM is around 0.65 and with the inclusion of nanopowder in higher concentrations the absorbance increased to 0.75. As a positive sign, when the increase in absorbance of the composite sample of PCM with Gr:Ag, the transmissibility decreases as shown in Figure 6. It was found that the addition of nanoparticles decreased the transmission and increased the absorbance. The decrease in light transmission may be attributed to the light absorption of the graphene nanoparticles.

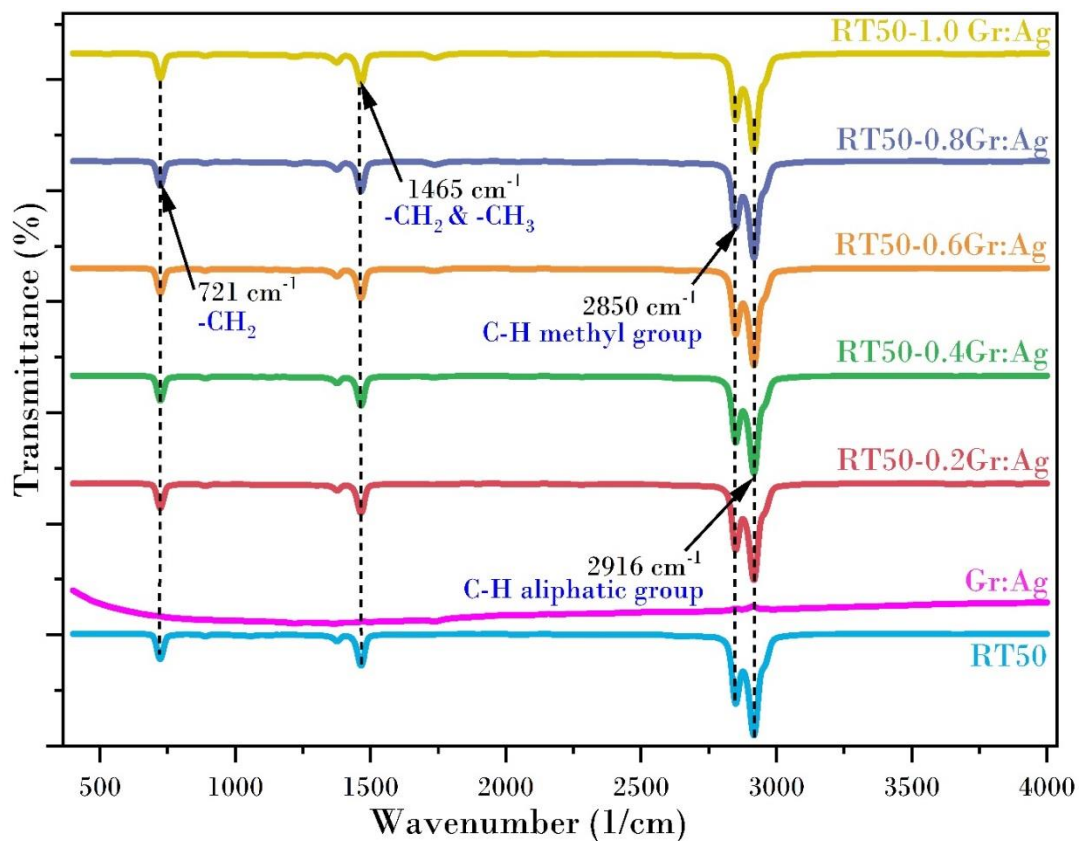


Figure 4. Functional group spectral curve of composite PCM from FTIR.

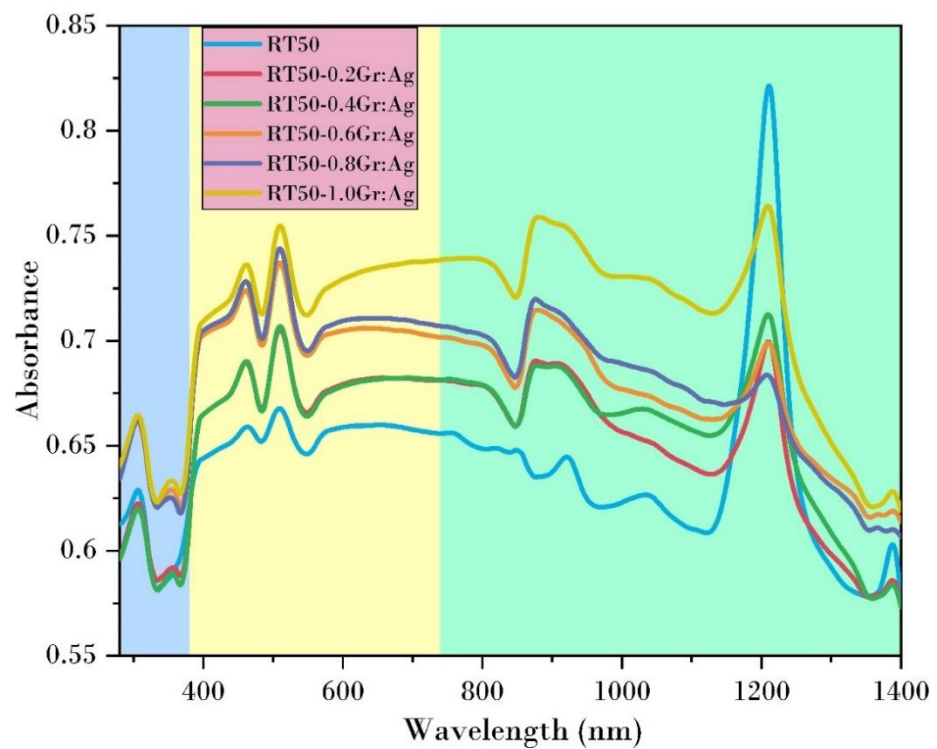


Figure 5. Solar spectral absorbance curve of the composite PCM characterized using UV-Vis spectroscopy.

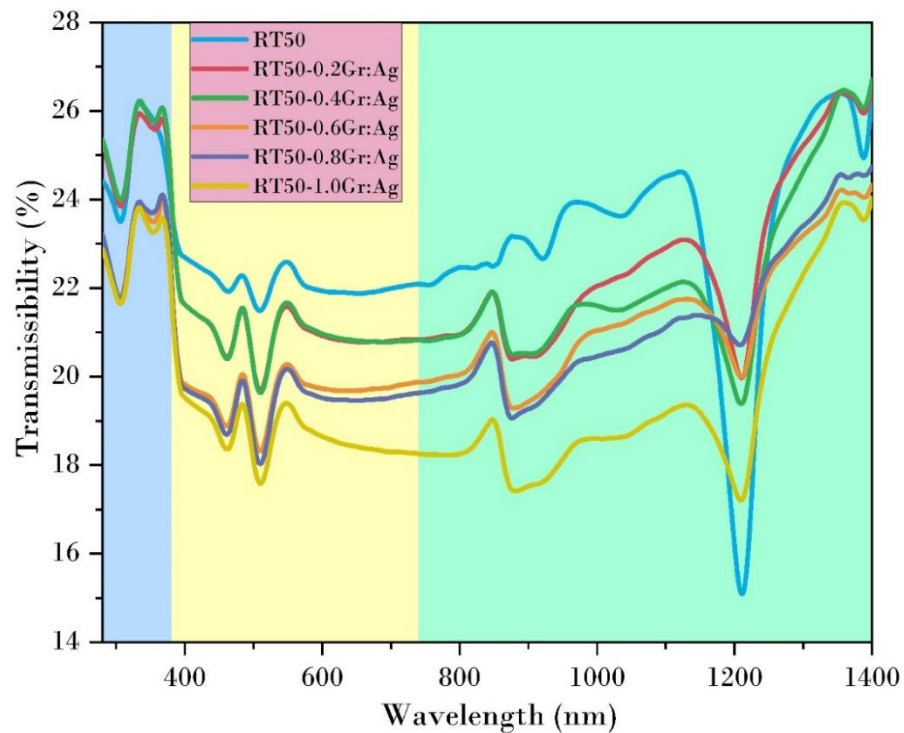


Figure 6. Solar spectral transmittance curve of the composite PCM characterized using UV-Vis spectroscopy.

The transmissibility of RT50 is determined to be 22.7%, whereas for composite PCM sample RT50-0.2Gr:Ag, RT50-0.4Gr:Ag, RT50-0.6Gr:Ag, RT50-0.8Gr:Ag, and RT50-1.0Gr:Ag, the transmissibility values are 21.8%, 21.6%, 20.4%, 20.2%, and 19.1%, respectively. As transmissibility and absorbance are inversely proportional, the reduction in transmission nature of RT50 using Gr:Ag is rewarded by an increase in absorbance. Higher absorptivity helps it respond better to the input solar radiation and contributes to higher thermal energy storage at a comparatively faster rate.

3.4. Thermal Conductivity

Though PCM offers numerous favorable thermal properties, the low thermal conductivity of PCM adversely affects the conductive nature of PCM. Using a dual-needle probe SH-3 TEMPOS thermal analyzer, the thermal conductivity of all composite samples RT50-0.2Gr:Ag, RT50-0.4Gr:Ag, RT50-0.6Gr:Ag, RT50-0.8Gr:Ag, and RT50-1.0Gr:Ag were determined. An average of ten values were taken for each sample to obtain the thermal conductivity values. Thermal conductivity of the nanopowder dispersed composite organic PCM was determined at a constant temperature of 20 °C because thermal conductivity is a temperature dependent parameter. Figure 7a illustrates the thermal conductivity obtained for a base PCM and the graphene silver doped composite PCM varies from 0.212 W/mK to 0.326 W/mK when Gr:Ag nanoparticle varies from 0.2 wt% to 0.8 wt%. With an increase in the volume fraction of graphene silver nanopowder, the thermal conductivity of the nanocomposite organic PCM adopts an increasing trend in a nonlinear fashion. The only possible mode of heat transfer within a PCM during the solid state is conduction; therefore, formation of well-developed thermal networks are significant, as shown in Figure 7b, for enhancing the thermal conductivity nature of an organic PCM to support fast charging.

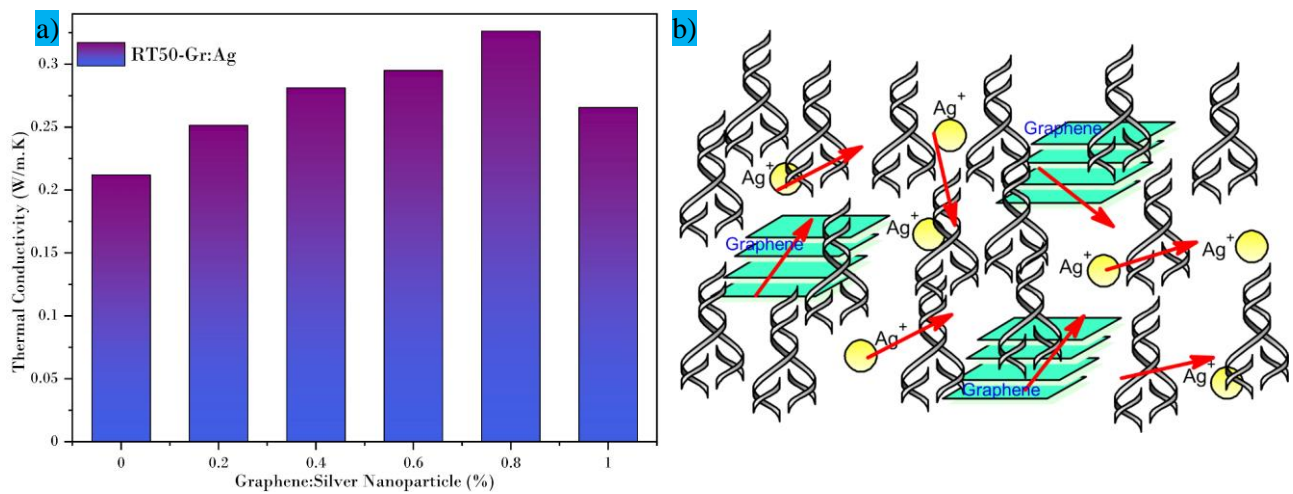


Figure 7. (a) Thermal conductivity of composite RT50 PCM with different weight% of Gr:Ag nanopowder. (b) Heat-transfer mechanism in organic PCM with hybrid nanoparticles.

The thermal conductivity of Gr:Ag composite PCM during the phase transition is ascribed to the phonon transfer occurring via phonon vibration. During the low-weight fraction of Gr:Ag nanopowder, the coupling of nanoparticles may not occur and does not form an established thermal network; however, with increased nanopowder, well-developed continuous thermal networks are formed and the thermal conductivity increases significantly. In addition, the surface area of the Gr nanopowder selected is 500–1200 m²/g, thereby providing interconnected networks for the heat transfer pathway [21]. With higher concentration of Gr:Ag, the mean path of the phonons is reduced by phenomena such as (a) phonon–phonon scattering and (b) phonon–impurity scattering [32]. The aforementioned scattering tends to decrease the thermal path with the organic PCM and contributes to lower thermal conductivity at higher concentrations. With higher concentrations of nanopowder, the nanoparticle results in excessive clustering resulting in agglomeration and sedimentation, which is a negative effect, as the PCMs are preferred because of their reliability over an extended number of thermal cycle changes from solid to liquid and vice versa.

3.5. Heating Enthalpy

Potential of a PCM to store heat energy is evaluated using a DSC instrument. Figure 8 depicts the heating enthalpy curve of PCMs and the Ag nanoparticle dispersed composite PCMs at different compositions. When nanoparticles are dispersed with a PCM, some fraction of the PCM is replaced with nanoparticles and their latent heat value tends to decrease. Similarly, the heating enthalpy plots of all the composite PCMs in Figure 8 replicate a minor change in latent heat value, which can be ascribed to the fraction of the PCM that is replaced by a fraction of a nanoparticle. However, a keen observation makes it clear that the drop in latent heat value is less than 3%. In contrast, the RT50-0.8Gr:Ag composite with a higher thermal conductivity has a tendency to offer latent heat values equal to the base PCM, which is because of the strong intermolecular bonding between nanoparticle and the PCM, which tends to absorb more energy to undergo phase transition and store them. The variation in phase transition temperatures of the PCM and the composite PCM is negligible, which does not distress the application of integrating PCM with various real time fields. The melting point increment is due to the higher melting point value of the hybrid Gr: Ag nanoparticle. By means of increasing the concentration of nanoparticles, the thermal barrier development is due to the higher melting point of nanoparticles that increases and leads to a minor increase in the PCM composite melting point. This also ensures the better thermal stability of the PCM. Variations in

phase transition temperature of the composite PCM are also ascribed to inappropriate crystallization during the phase change.

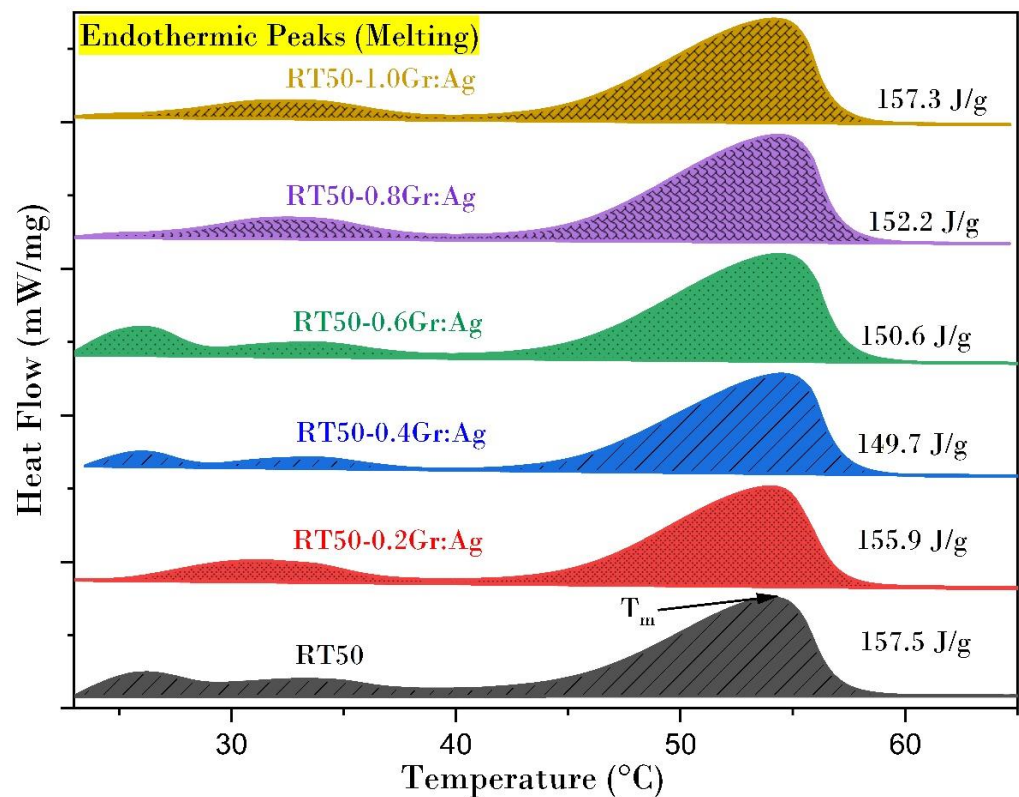


Figure 8. Heating enthalpy curve of PCMs and PCM composites.

PCMs store thermal energy during phase transition. When heat input is supplied, the PCM melts and changes state from solid to liquid. During this phase transition, the supplied heat energy is stored and results in an endothermic peak. Similarly, it is more important for the PCM to release the stored energy for further usages because PCMs are thermal batteries. When the work environment temperature goes below the temperature of the PCM, the heat is liberated with a change in state of the PCM from liquid to solid. During this phase transition, the stored heat energy is liberated, and it results in exothermic peaks. In terms of degree of supercooling, organic PCMs are superior to inorganic PCMs because they freeze at their melting point and ensure complete liberation of the stored heat energy [33].

3.6. Thermal Degradation Evaluation

Thermal stability of the organic PCM RT50 and Gr:Ag composite was assessed using TGA by evaluating the loss in weight percentage of the sample with and increase in temperature. Weight degradation of pure RT50 and its composite (RT50-0.2Gr:Ag, RT50-0.4Gr:Ag, RT50-0.6Gr:Ag, RT50-0.8Gr:Ag, and RT50-1.0Gr:Ag) are displayed in Figure 9. It can be inferred from Figure 8 that no decomposition of samples is noticed up to 200 °C, and the maximum decomposition (about 90%) is observed between the temperature range of 230 °C to 300 °C as the PCM tends to evaporate and degrade at this point. Decomposition initiation point of all the composite samples resembles that of the base organic RT50 PCM; however, with Gr:Ag nanopowder, the decomposition culmination point is further extended up to 310–330 °C with the presence of residual nanopowder. All composite samples degrade at a higher temperature compared to the base RT50 PCM; however, the sample RT50-1.0Gr:Ag depicts a minor decline in the degradation temperature. This decrease may be ascribed to the microcomposite formation due to the clustering of the

nanopowder. TGA curves endorse the effective dispersion of Gr:Ag nanopowder onto the PCM and thus the thermal stability of the samples is improved. This is in agreement with the conclusions described in earlier investigations [34,35].

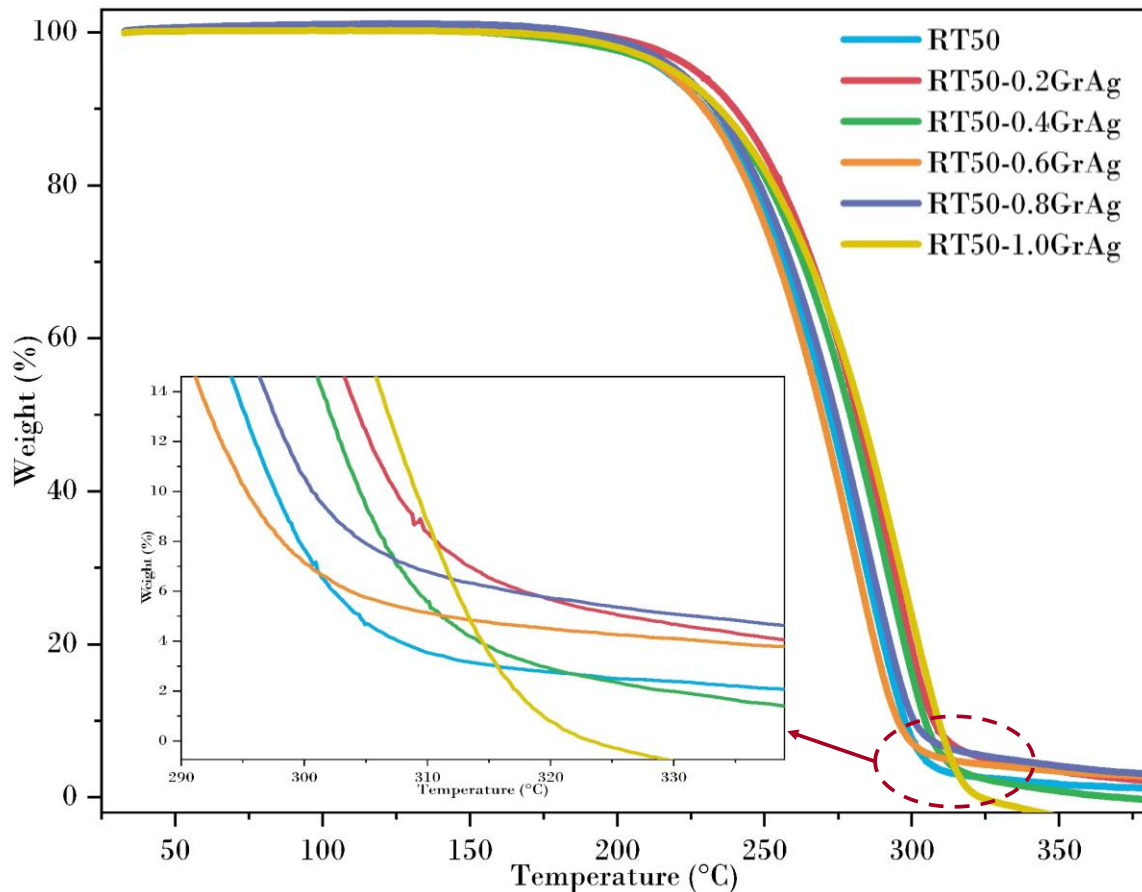


Figure 9. Thermal degradation analysis of composite RT50 PCM with different weight% of Gr:Ag nanopowder.

3.7. Thermal Cycling Analysis

To confirm the longstanding operation of RT50-0.8Gr:Ag composite sample, a thermal cycling test was conducted. Overall, thermal cycling tests are cost effective and save time because they provide evidence for the thermal consistency and reliability of the PCM over the long run, even before applying them for any specific application. In the current investigation, a customized thermal cycler machine with three compartments was used to run three samples instantaneously. Pure RT50 PCM and Gr:Ag dispersed composite RT50-0.8Gr:Ag (used due to the high thermal conductivity) were operated under the thermal cycler machine to assess the thermal stability after 500 cycles. A total of 3 gm of pure and composite samples were taken in a container, which was heated to a maximum of 80 °C (storing thermal energy) and cooled down to 35 °C (releasing thermal energy) to confirm complete phase transition. After 500 thermal cycles of the charging and discharging process, the composite samples were visualized using SEM before being characterized using FTIR, TGA, and DSC devices to realize the chemical and thermal stability. SEM images in Figure 10a,b confirmed that the RT50 PCM and RT50-0.8GrAg composite PCM exhibit a steady scattering of Gr:Ag nanoparticles without any chemical reaction involving the PCM molecule. Homogeneously dispersed Gr:Ag nanoparticles in Figure 10b are vital for better thermal properties as they provide thermal networks, and do not agglomerate. Microsized layers of graphene molecules and nanosized spherical silver molecules are marked for better thoughtfulness. Chemical stability of the base PCM and composite PCM

are established through the FTIR spectral curve, as shown in Figure 10c. The sample exhibits four vibration peaks at wavenumbers 2916 cm^{-1} , 2848 cm^{-1} , 1465 cm^{-1} , and 717 cm^{-1} , which is similar to the peaks observed before conducting any thermal cycles. The peaks are in close resemblance and agreement with the peaks obtained before conducting any thermal cycles. Furthermore, it is useful to see no shifts in the peak position after 500 thermal cycles because this specifies no variation in electronic distribution and hybridization. From the above discussion, it can be decided that this composite PCM would offer a robust nature when applied to real-time applications. For better consideration for the readers, we have also provided a digital image of the composite PCM before and after 500 thermal cycles in Figure 10d.

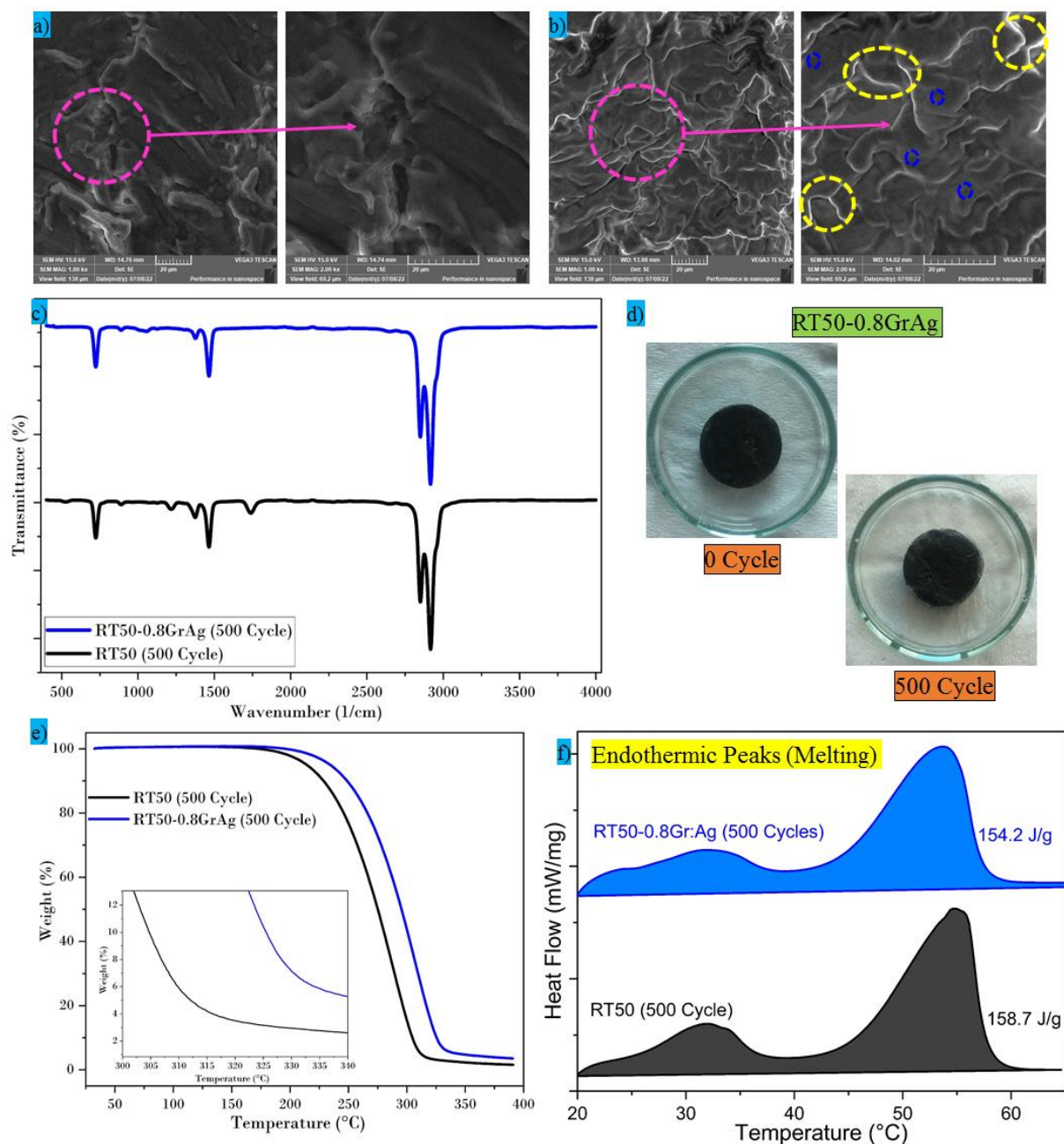


Figure 10. Thermal cycling analysis after 500 cycles. (a) SEM image of RT50 PCM, (b) SEM image of RT50-0.8GrAg PCM, (c) FTIR spectral analysis, (d) digital image of composite PCM before and after 500 thermal cycles, (e) thermal decomposition analysis, and (f) heating enthalpy comparison.

Figure 10e depicts the thermal stability of the PCM, where we are able to explore the volatile component fraction present in the composite and the weight loss percentage of PCMs with increases in temperature. Decomposition temperature of the PCM and composite PCM after 500 thermal cycles depicts an increase in decomposition temperature; this phenomenon is observed because of repeated change of PCM temperature. Higher decomposition temperatures of the PCM after thermal cycling test are an encouraging sign for operating the PCM for more charging and discharging sequences. Figure 10f shows the phase transition temperature and change in melting enthalpy of the base PCM and composite PCM after conducting 500 thermal cycle tests. With continuous charging and discharging operations at different temperatures, the materials tend to degrade, which can be ascribed to the absorption of moisture content and impurities from external ambient conditions [36]. These ambient conditions and higher temperatures are expected to lead to strange behaviors of the PCMs when they are tested with DSC. Variations in phase transition temperatures of the composite PCMs are observed because of inappropriate crystallization during the phase changes. After complete melting and phase transition from solid to liquid, the crystal structure of the PCMs changes and the thermophysical properties of the sample changes.

4. Conclusions

In the current experimental study, five sample of graphene silver hybrid nanoparticle dispersed composite organic PCMs were prepared at weight concentrations of 0.2, 0.4, 0.6, 0.8, and 1.0. All the hybrid nanoparticle dispersed composite PCMs were investigated to understand their morphological and microstructure behavior, chemical stability, optical absorptivity, and thermal physical properties with thermal cycling tests. Noteworthy conclusions of the current research investigation are consolidated below:

- SEM images ensure the uniform dispersion of hybrid nanoparticles within the PCM matrix, which provides evidence that the thermal networks facilitated effective heat transfer.
- The addition of the hybrid nanoparticle Gr:Ag leads to an increase in thermal conductivity of the base organic PCM from 0.212 W/mK to 0.326 W/mK, which is considerably about 53.77% higher due to the well-developed thermal networks and phonon–phonon interaction.
- The latent heat value of the composite PCM is slightly reduced when hybrid nanoparticles form a fraction of the PCM volume that is occupied by the nanoparticles. The drop in latent heat value is considerably lower. Thermal decomposition temperature of the PCMs is slightly enhanced by nanoparticles.
- The thermal decomposition of the composite samples was analyzed using TGA, where the decomposition temperature of the hybrid nanoparticle dispersed PCM were substantially increased compared to the base PCMs. With higher dispersion of the nanoparticles, there was a reduction in the decomposition temperature.
- Gr:Ag dispersed at a 0.8 wt% with PCM exhibits decent chemical and thermal stability after 500 cycles. Spectral peaks are constant before and after the thermal cycles, the decomposition points are further increased after the thermal cycling tests, and the latent heat value is almost the same before and after the thermal cycles, which indicates the PCMs suitability for energy storage applications.

From the obtained results, it can be seen that the dispersion of the hybrid nanoparticle with a PCM at a 0.8% weight concentration ratio exhibits better chemical, optical, and thermal energy storage characteristics. In addition, we also recommend the usage of this composite PCM for any thermal system that generates waste heat at low temperatures.

Author Contributions: Conceptualization, B.K. and A.K.P.; Data curation, B.K.; Formal analysis, B.K. and A.Y.; Funding acquisition, S.R.; Investigation, B.K., A.K.P. and V.V.T.; Methodology, B.K.; Project administration, A.K.P., S.R. and M.S.; Resources, A.K.P.; Supervision, S.R., M.S. and V.V.T.; Validation, B.K.; Writing—original draft, B.K. and A.Y.; Writing—review & editing, A.K.P. and V.V.T. All authors have read and agreed to the published version of the manuscript.

Funding: This research has been funded by Sunway University through Sunway University's Internal Grant Scheme 2022 (GRTIN-IGS-RCNMET[S]-15-2022)) for conducting this research.

Institutional Review Board Statement: Not Applicable.

Informed Consent Statement: Not Applicable.

Data Availability Statement: The data presented in this study is available within the article.

Acknowledgments: All authors duly acknowledges the laboratory support and assistance of Sunway University for conducting the current research investigation.

Conflicts of Interest: The authors declare no conflict of interest.

Abbreviations

Composite Code

RT50	Rubitherm organic PCM with melting point 50 °C
Gr:Ag	Graphene silver nanopowder
RT50-0.2Gr:Ag	RT50 with 0.2% Gr:Ag nanopowder
RT50-0.4Gr:Ag	RT50 with 0.4% Gr:Ag nanopowder
RT50-0.6Gr:Ag	RT50 with 0.6% Gr:Ag nanopowder
RT50-0.8Gr:Ag	RT50 with 0.8% Gr:Ag nanopowder
RT50-1.0Gr:Ag	RT50 with 1.0% Gr:Ag nanopowder

References

- Smith, J.B.; Schneider, S.H.; Oppenheimer, M.; Yohe, G.W.; Hare, W.; Mastrandrea, M.D.; Patwardhan, A.; Burton, I.; Corfee-Morlot, J.; Magadza, C.H. Assessing dangerous climate change through an update of the Intergovernmental Panel on Climate Change (IPCC) "reasons for concern". *Proc. Natl. Acad. Sci. USA* **2009**, *106*, 4133–4137. [[CrossRef](#)] [[PubMed](#)]
- Laghari, I.A.; Samykano, M.; Pandey, A.; Kadirgama, K.; Mishra, Y.N. Binary composite (TiO₂-Gr) based nano-enhanced organic phase change material: Effect on thermophysical properties. *J. Energy Storage* **2022**, *51*, 104526. [[CrossRef](#)]
- Tariq, S.L.; Ali, H.M.; Akram, M.A.; Janjua, M.M.; Ahmadlouydarab, M. Nanoparticles enhanced phase change materials (NePCMs)-A recent review. *Appl. Therm. Eng.* **2020**, *176*, 115305. [[CrossRef](#)]
- Sun, K.; Kou, Y.; Zhang, Y.; Liu, T.; Shi, Q. Photo-triggered hierarchical porous carbon-based composite phase-change materials with superior thermal energy conversion capacity. *ACS Sustain. Chem. Eng.* **2020**, *8*, 3445–3453. [[CrossRef](#)]
- Zhang, Y.; Li, X.; Li, J.; Ma, C.; Guo, L.; Meng, X. Solar-driven phase change microencapsulation with efficient Ti₄O₇ nanoconverter for latent heat storage. *Nano Energy* **2018**, *53*, 579–586. [[CrossRef](#)]
- Chen, R.; Yao, R.; Xia, W.; Zou, R. Electro/photo to heat conversion system based on polyurethane embedded graphite foam. *Appl. Energy* **2015**, *152*, 183–188. [[CrossRef](#)]
- Yang, J.; Qi, G.-Q.; Liu, Y.; Bao, R.-Y.; Liu, Z.-Y.; Yang, W.; Xie, B.-H.; Yang, M.-B. Hybrid graphene aerogels/phase change material composites: Thermal conductivity, shape-stabilization and light-to-thermal energy storage. *Carbon* **2016**, *100*, 693–702. [[CrossRef](#)]
- Chen, L.; Zou, R.; Xia, W.; Liu, Z.; Shang, Y.; Zhu, J.; Wang, Y.; Lin, J.; Xia, D.; Cao, A. Electro-and photodriven phase change composites based on wax-infiltrated carbon nanotube sponges. *ACS Nano* **2012**, *6*, 10884–10892. [[CrossRef](#)]
- Li, Y.; Samad, Y.A.; Polychronopoulou, K.; Alhassan, S.M.; Liao, K. From biomass to high performance solar-thermal and electric-thermal energy conversion and storage materials. *J. Mater. Chem. A* **2014**, *2*, 7759–7765. [[CrossRef](#)]
- Wang, Y.; Tang, B.; Zhang, S. Visible light-driven organic form-stable phase change materials for solar energy storage. *RSC Adv.* **2012**, *2*, 5964–5967. [[CrossRef](#)]
- Awad, S.A.; Khalaf, E.M. Improvement of the chemical, thermal, mechanical and morphological properties of polyethylene terephthalate-graphene particle composites. *Bull. Mater. Sci.* **2018**, *41*, 67. [[CrossRef](#)]
- Nan, H.Y.; Ni, Z.H.; Wang, J.; Zafar, Z.; Shi, Z.X.; Wang, Y.Y. The thermal stability of graphene in air investigated by Raman spectroscopy. *J. Raman Spectrosc.* **2013**, *44*, 1018–1021. [[CrossRef](#)]
- Xu, M.; Liang, T.; Shi, M.; Chen, H. Graphene-like two-dimensional materials. *Chem. Rev.* **2013**, *113*, 3766–3798. [[CrossRef](#)] [[PubMed](#)]
- Gao, Y.; Hao, P. Mechanical properties of monolayer graphene under tensile and compressive loading. *Phys. E: Low-Dimens. Syst. Nanostruct.* **2009**, *41*, 1561–1566. [[CrossRef](#)]
- Jamil, N.; Kaur, J.; Pandey, A.; Shahabuddin, S.; Hassani, S.; Saidur, R.; Ali, R.R.; Sidik, N.A.C.; Naim, M. A review on nano enhanced phase change materials: An enhancement in thermal properties and specific heat capacity. *J. Adv. Res. Fluid Mech. Therm. Sci.* **2019**, *57*, 110–120.
- Jouhara, H.; Żabnieńska-Góra, A.; Khordehghah, N.; Ahmad, D.; Lipinski, T. Latent thermal energy storage technologies and applications: A review. *Int. J. Thermofluids* **2020**, *5*, 100039. [[CrossRef](#)]

17. Li, W.; Guo, S.; Tan, L.; Liu, L.; Ao, W. Heat transfer enhancement of nano-encapsulated phase change material (NEPCM) using metal foam for thermal energy storage. *Int. J. Heat Mass Transf.* **2021**, *166*, 120737. [[CrossRef](#)]
18. Abdelrazik, A.; Saidur, R.; Al-Sulaiman, F.; Al-Ahmed, A.; Ben-Mansour, R. Multiwalled CNT and graphene nanoplatelets based nano-enhanced PCMs: Evaluation for the thermal performance and its implications on the performance of hybrid PV/thermal systems. *Mater. Today Commun.* **2022**, *31*, 103618. [[CrossRef](#)]
19. Li, Y.; Sun, K.; Kou, Y.; Liu, H.; Wang, L.; Yin, N.; Dong, H.; Shi, Q. One-step synthesis of graphene-based composite phase change materials with high solar-thermal conversion efficiency. *Chem. Eng. J.* **2022**, *429*, 132439. [[CrossRef](#)]
20. Vivekananthan, M.; Amirtham, V.A. Characterisation and thermophysical properties of graphene nanoparticles dispersed erythritol PCM for medium temperature thermal energy storage applications. *Thermochim. Acta* **2019**, *676*, 94–103. [[CrossRef](#)]
21. Liu, Y.; Zheng, R.; Tian, T.; Li, J. Characteristics of thermal storage heat pipe charged with graphene nanoplatelets enhanced organic phase change material. *Energy Convers. Manag.* **2022**, *267*, 115902. [[CrossRef](#)]
22. Tariq, S.L.; Ali, H.M.; Akram, M.A.; Janjua, M.M. Experimental investigation on graphene based nanoparticles enhanced phase change materials (GbNePCMs) for thermal management of electronic equipment. *J. Energy Storage* **2020**, *30*, 101497. [[CrossRef](#)]
23. Pasupathi, M.K.; Alagar, K.; Mm, M.; Aritra, G. Characterization of hybrid-nano/paraffin organic phase change material for thermal energy storage applications in solar thermal systems. *Energies* **2020**, *13*, 5079. [[CrossRef](#)]
24. Pradeep, N.; Paramasivam, K.; Rajesh, T.; Purusothamanan, V.S.; Iyahrja, S. Silver nanoparticles for enhanced thermal energy storage of phase change materials. *Mater. Today: Proc.* **2021**, *45*, 607–611. [[CrossRef](#)]
25. Prabhu, B.; ValanArasu, A. Stability analysis of TiO₂-Ag nanocomposite particles dispersed paraffin wax as energy storage material for solar thermal systems. *Renew. Energy* **2020**, *152*, 358–367.
26. Zhan, W.; Zhao, Y.; Yuan, Y.; Yi, H.; Song, S. Development of 2D-Mt/SA/AgNPs microencapsulation phase change materials for solar energy storage with enhancement of thermal conductivity and latent heat capacity. *Sol. Energy Mater. Sol. Cells* **2019**, *201*, 110090. [[CrossRef](#)]
27. Wen, R.; Zhu, S.; Wu, M.; Chen, W. Design and preparation of Ag modified expanded graphite based composite phase change materials with enhanced thermal conductivity and light-to-thermal properties. *J. Energy Storage* **2021**, *41*, 102936. [[CrossRef](#)]
28. Qian, T.; Li, J.; Min, X.; Guan, W.; Deng, Y.; Ning, L. Enhanced thermal conductivity of PEG/diatomite shape-stabilized phase change materials with Ag nanoparticles for thermal energy storage. *J. Mater. Chem. A* **2015**, *3*, 8526–8536. [[CrossRef](#)]
29. Luo, W.; Hu, X.; Che, Y.; Zu, S.; Li, Q.; Jiang, X.; Liu, D. Form-stable phase change materials enhanced photothermic conversion and thermal conductivity by Ag-expanded graphite. *J. Energy Storage* **2022**, *52*, 105060. [[CrossRef](#)]
30. Li, Y.; Li, Y.; Huang, X.; Zheng, H.; Lu, G.; Xi, Z.; Wang, G. Graphene-CoO/PEG composite phase change materials with enhanced solar-to-thermal energy conversion and storage capacity. *Compos. Sci. Technol.* **2020**, *195*, 108197. [[CrossRef](#)]
31. Kalidasan, B.; Pandey, A.; Shahabuddin, S.; George, M.; Sharma, K.; Samykano, M.; Tyagi, V.; Saidur, R. Synthesis and characterization of conducting Polyaniline@ cobalt-Paraffin wax nanocomposite as nano-phase change material: Enhanced thermophysical properties. *Renew. Energy* **2021**, *173*, 1057–1069.
32. Fikri, M.A.; Pandey, A.; Samykano, M.; Kadirgama, K.; George, M.; Saidur, R.; Selvaraj, J.; Abd Rahim, N.; Sharma, K.; Tyagi, V. Thermal conductivity, reliability, and stability assessment of phase change material (PCM) doped with functionalized multi-wall carbon nanotubes (FMWCNTs). *J. Energy Storage* **2022**, *50*, 104676. [[CrossRef](#)]
33. Kalidasan, B.; Pandey, A.; Saidur, R.; Samykano, M.; Tyagi, V. Nano additive enhanced salt hydrate phase change materials for thermal energy storage. *Int. Mater. Rev.* **2022**, *1–44*. [[CrossRef](#)]
34. Yousefi, A.; Tang, W.; Khavarian, M.; Fang, C. Development of novel form-stable phase change material (PCM) composite using recycled expanded glass for thermal energy storage in cementitious composite. *Renew. Energy* **2021**, *175*, 14–28. [[CrossRef](#)]
35. Balaji, A.; Saravanan, R.; Purushothaman, R.; Vijayaraj, S.; Balasubramanian, P. Investigation of Thermal Energy Storage (TES) with lotus stem biocomposite block using PCM. *Clean. Eng. Technol.* **2021**, *4*, 100146. [[CrossRef](#)]
36. Anand, A.; Shukla, A.; Kumar, A.; Buddhi, D.; Sharma, A. Cycle test stability and corrosion evaluation of phase change materials used in thermal energy storage systems. *J. Energy Storage* **2021**, *39*, 102664. [[CrossRef](#)]